Adv Comput Math (2022) 48:41
https://doi.org/10.1007/s10444-022-09962-2

High-order conservative energy quadratization schemes for the Klein-Gordon-Schrödinger equation

Xin Li[1] · **Luming Zhang**[2]

Received: 31 August 2021 / Accepted: 27 May 2022 / Published online: 21 June 2022

Abstract

In this paper, we design two classes of high-accuracy conservative numerical algorithms for the nonlinear Klein-Gordon-Schrödinger system in two dimensions. By introducing the energy quadratization technique, we first transform the original system into an equivalent one, where the energy is modified as a quadratic form. The Gauss-type Runge-Kutta method and the Fourier pseudo-spectral method are then employed to discretize the reformulation system in time and space, respectively. The fully discrete schemes inherit the conservation of mass and modified energy and can reach high-order accuracy in both temporal and spatial directions. In order to complement the proposed schemes and speed up the calculation, we also develop another class of conservative schemes combined with the prediction-correction technique. Numerous experimental results are reported to demonstrate the efficiency and high accuracy of the new methods.

Keywords Klein-Gordon-Schrödinger equation · Energy quadratization · Gauss-type Runge-Kutta method · Fourier pseudo-spectral method · Prediction-correction · Conservation

Mathematics Subject Classification (2010) 65Mxx

Communicated by: Tobin Driscoll

✉ Xin Li
xli_math@hfut.edu.cn

Luming Zhang
zhanglm@nuaa.edu.cn

[1] School of Mathematics, Hefei University of Technology, Hefei, 230009, Anhui, People's Republic of China

[2] Department of Mathematics, Nanjing University of Aeronautics and Astronautics, Nanjing, 210016, Jiangsu, People's Republic of China

1 Introduction

The Klein-Gordon-Schrödinger (KGS) equation is a significant model in quantum field theory, which is used to describe the interaction between conserved complex neutron field and neutral meson through Yukawa coupling [1, 2]. In this work, we investigate the following dimensionless KGS system

$$\mathrm{i}\psi_t(\mathbf{x},t)+\frac{1}{2\alpha}\nabla^2\psi(\mathbf{x},t)+\psi(\mathbf{x},t)\phi(\mathbf{x},t)=0 \qquad \text{for } \mathbf{x}\in\Omega \text{ and } 0<t\le T, \quad (1.1)$$

$$\phi_{tt}(\mathbf{x},t)-\nabla^2\phi(\mathbf{x},t)+\beta^2\phi(\mathbf{x},t)-|\psi(\mathbf{x},t)|^2=0 \qquad \text{for } \mathbf{x}\in\Omega \text{ and } 0<t\le T, \quad (1.2)$$

$$(\psi,\phi,\phi_t)(\mathbf{x},0)=(\psi_0,\phi_0,\phi_1)(\mathbf{x}) \qquad \text{for } \mathbf{x}\in\bar{\Omega}, \quad (1.3)$$

where $\mathbf{x}=(x,y)^T$ and t is time. $\Omega=(x_1,x_2)\times(y_1,y_2)$ is a bounded domain and $\bar{\Omega}$ represents its closure. $\nabla^2=\Delta$ is the two-dimensional Laplacian operator. The unknown functions ψ and ϕ denote a complex scalar nucleon field and a real scalar meson field, respectively. α is a positive constant and β is a real constant describes the ratio of mass between a meson and a nucleon. ψ_0 is a given complex-valued function and ϕ_0 and ϕ_1 are two given real-valued functions. Together with the periodic boundary conditions, it is straightforward to confirm that the periodic initial value problem possess two conservation laws corresponding to the total mass

$$\frac{\mathrm{d}M}{\mathrm{d}t}=0 \quad \text{with} \quad M[\psi]=\int_\Omega |\psi(\mathbf{x},t)|^2\,\mathrm{d}\mathbf{x}, \quad (1.4)$$

and the energy

$$\frac{\mathrm{d}E}{\mathrm{d}t}=0 \quad \text{with} \quad E[\psi,\phi]=\frac{1}{2}\int_\Omega \Big(\frac{1}{\alpha}|\nabla\psi|^2+|\nabla\phi|^2+|\phi_t|^2+\beta^2|\phi|^2-2\phi|\psi|^2\Big)\,\mathrm{d}\mathbf{x}. \quad (1.5)$$

Extensive mathematical and numerical studies are carried out in the literature. On the one hand, Fukuda et al. [3] establish the existence and uniqueness of global smooth solution for the KGS equation. In [4–6], the well-posedness and asymptotic behavior are shown. For the singular limits, periodic wave solutions and solitary waves, we refer to [7, 8] and the references therein. On the other hand, a variety of numerical methods are employed to solve the KGS equation efficiently, including the finite difference method [9–11], the Galerkin finite element method [12], the symplectic and multi-symplectic method [13, 14], the spectral and pseudo-spectral method [2, 15, 16] and the orthogonal spline collocation method [17], etc. Most of the proposed methods admit the conservation properties at the discrete time level, which could avoid the nonlinear blow-up essentially and capture the dynamics of PDE model precisely. Although the existing methods have commendably achieved the high-order accuracy in space, to the best of our knowledge, these structure-preserving schemes have only second-order accuracy in time. Few references consider the temporal higher-order conservative algorithms for the KGS system, which leads to the restriction of using large time steps in numerical implementation.

Runge-Kutta (RK) method is a classical method which is applied to solve ODE numerically. It is well known that all RK methods preserve arbitrary linear invariants, and the symplectic RK (SRK) methods preserve arbitrary quadratic invariants

[18, 19]. More specially, if we take the SRK coefficients $c_1, \ldots, c_s$ as the nodes of Gaussian quadrature formula, it yields Gauss-type RK (GRK) method or Gauss collocation method [20]. Since the RK methods are unable to guarantee all polynomial invariants of degree higher than two [21], it is therefore a great challenge to develop high-order energy-conserving schemes via the RK methods.

Most recently, the energy quadratization (EQ) strategy is presented and widely utilized to the gradient flow models. One is the invariant energy quadratization (IEQ) approach [22–24], which can be seen as a generalization of Lagrange multiplier method or auxiliary variable method originally. It transforms the energy into a quadratic form by adopting a new variable, and then reformulate the primal problem into an equivalent system which inherits a modified energy conservation law. The other is the so-called scalar auxiliary variable (SAV) approach which is proposed by Shen et al. [25, 26] as a modification to the former. It overcomes some shortcomings of IEQ and make the implementation more simple and efficient. Interested readers are referred to the review paper [27] for more details. Enlightened by this EQ strategy, a family of arbitrarily high-order, unconditionally energy stable GRK schemes are presented for the gradient flow models [28–30]. The authors illustrate that these schemes inherit the energy dissipation property and show excellent numerical stability even with a relatively large time step. More importantly, this seminal idea could be generalized and utilized to any gradient flow models. On the other hand, with the help of EQ approach, a variety of second-order energy-preserving schemes are developed for the conservative system [31, 32]. Higher-order energy-preserving algorithms are also designed in [33, 34]. In this work, we employ the EQ methodology and strive to construct two classes of conservative algorithms for solving the KGS model numerically.

The rest of this paper is arranged as follows. In Section 2, we introduce the EQ technique for the KGS equation and derive the EQ reformulation system equivalently. Two conservation laws of this new system are demonstrated at the same time. The GRK method and the Fourier pseudo-spectral method are employed in the next section to discretize the transformed system in time and space, respectively. We then develop a class of fully discrete high-order EQ schemes which maintain two invariants at the discrete time level. In order to accelerate the calculations and improve the accuracy as well as the stability, in Section 4, we incorporate the prediction-correction (PC) technique and design another class of high-order energy-preserving EQ-PC algorithms for this problem. It is worthy to emphasize that these strategies could be extended and used to other conservative equations for developing high-order structure-preserving schemes. In Section 5, several numerical examples are provided to illustrate the performances of the suggested schemes, followed by some concluding remarks in the last section.

2 Energy quadratization reformulation

In order to provide a graceful platform for high-accuracy numerical discretization, in this section, we reformulate the KGS equation into an equivalent system by incorporating the method of order reduction and the EQ technique. New system retains the

mass and modified energy invariants. We set $\psi = p + \mathrm{i}q$ and rewrite (1.1) as a pair of real-valued equations. Moreover, the method of order reduction in time is applied to (1.2). After that the KGS system implies that

$$\begin{cases} p_t = -\frac{1}{2\alpha}\Delta q - q\phi, \\ q_t = \frac{1}{2\alpha}\Delta p + p\phi, \\ \phi_t = \omega, \\ \omega_t = \Delta\phi - \beta^2\phi + (p^2+q^2). \end{cases} \tag{2.1}$$

The corresponding mass and energy functionals (1.4)–(1.5) yield

$$M[p,q] = \int_\Omega (p^2+q^2)\,\mathrm{d}\mathbf{x}, \tag{2.2}$$

$$E[p,q,\phi,\omega] = \frac{1}{2}\int_\Omega \Big(\frac{1}{\alpha}|\nabla p|^2 + \frac{1}{\alpha}|\nabla q|^2 + |\nabla\phi|^2 + |\omega|^2 + \beta^2|\phi|^2\Big)\,\mathrm{d}\mathbf{x} - \int_\Omega \phi(p^2+q^2)\,\mathrm{d}\mathbf{x}. \tag{2.3}$$

Set $F(\phi, p, q) = \phi(p^2+q^2)$ and define the continuous inner product $(u, v) := \int_\Omega u \cdot v\,\mathrm{d}\mathbf{x}$ with the associated L^2-norm $\|u\|_2 := \sqrt{(u,u)}$. We next introduce the EQ strategy to reformulate the aforementioned system (2.1). From [35, 36], it can be shown that $\int_\Omega F(\phi, p, q)\,\mathrm{d}\mathbf{x}$ is bounded if (ϕ, p, q) is a solution of (2.1). As a consequence, on the one hand, we utilize the IEQ approach by introducing an auxiliary variable

$$r(\mathbf{x}, t) = \sqrt{F(\phi, p, q) + C_0},$$

where C_0 is a constant large enough such that $F(\phi, p, q) + C_0 > 0$. The energy functional (2.3) could be rewritten as a quadratic form

$$E_{\mathrm{ieq}} = \frac{1}{2}\int_\Omega \Big(\frac{1}{\alpha}|\nabla p|^2 + \frac{1}{\alpha}|\nabla q|^2 + |\nabla\phi|^2 + |\omega|^2 + \beta^2|\phi|^2\Big)\,\mathrm{d}\mathbf{x} - \|r\|_2^2 + C_0|\Omega|. \tag{2.4}$$

Then, we reformulate system (2.1) into the following equivalent IEQ form

$$\begin{cases} p_t = -\frac{1}{2\alpha}\Delta q - \frac{r}{\sqrt{F(\phi,p,q)+C_0}}q\phi, \\ q_t = \frac{1}{2\alpha}\Delta p + \frac{r}{\sqrt{F(\phi,p,q)+C_0}}p\phi, \\ \phi_t = \omega, \\ \omega_t = \Delta\phi - \beta^2\phi + \frac{r}{\sqrt{F(\phi,p,q)+C_0}}(p^2+q^2), \\ r_t = \frac{1}{2\sqrt{F(\phi,p,q)+C_0}}\big(\phi_t(p^2+q^2) + 2\phi(pp_t + qq_t)\big), \end{cases} \tag{2.5}$$

with the consistent initial condition

$$(p,q,\phi,\omega)(\mathbf{x},0) = \big(\mathrm{Re}(\psi_0), \mathrm{Im}(\psi_0), \phi_0, \phi_1\big),\ r(\mathbf{x},0) = \sqrt{F(\phi,p,q)|_{t=0} + C_0} \quad \text{for } \mathbf{x} \in \bar{\Omega}.$$

Theorem 2.1 *The IEQ reformulated system* (2.5) *satisfies two conservation laws corresponding to the mass and energy defined in* (2.2) and (2.4)*, respectively.*

Proof From (2.2), it is readily to check that

$$\frac{\mathrm{d}M}{\mathrm{d}t} = 2(p,\, p_t) + 2(q,\, q_t) = 0, \tag{2.6}$$

where the first two relations of (2.5) were used. The conservation of total mass is accomplished. Moreover, we utilize the variational derivative and obtain

$$\begin{aligned}\frac{\mathrm{d}E_{\mathrm{ieq}}}{\mathrm{d}t} &= \left(\frac{\delta E_{\mathrm{ieq}}}{\delta p},\, p_t\right) + \left(\frac{\delta E_{\mathrm{ieq}}}{\delta q},\, q_t\right) + \left(\frac{\delta E_{\mathrm{ieq}}}{\delta \phi},\, \phi_t\right) + \left(\frac{\delta E_{\mathrm{ieq}}}{\delta \omega},\, \omega_t\right) + \left(\frac{\delta E_{\mathrm{ieq}}}{\delta r},\, r_t\right)\\ &= \left(-\frac{1}{\alpha}\Delta p,\, p_t\right) + \left(-\frac{1}{\alpha}\Delta q,\, q_t\right) + (-\Delta\phi + \beta^2\phi,\, \phi_t) + (\omega,\, \omega_t) - (2r,\, r_t).\end{aligned}$$

Substituting (2.5) into the right-hand side of the above equality gives zero. This proves the IEQ reformulated system conserves a similar quadratic energy conservation law and completes the proof of this theorem. □

On the other hand, we employ the SAV approach to obtain another EQ reformulation, by incorporating a scalar auxiliary variable

$$k(t) = \sqrt{\big(F(\phi,\, p,\, q),\, 1\big) + C_0},$$

where C_0 is similarly defined so that to make k well-posed. In this case, the nonlinear energy functional (2.3) is rewritten as

$$E_{\mathrm{sav}} = \frac{1}{2}\int_\Omega \Big(\frac{1}{\alpha}|\nabla p|^2 + \frac{1}{\alpha}|\nabla q|^2 + |\nabla\phi|^2 + |\omega|^2 + \beta^2|\phi|^2\Big)\,\mathrm{d}\mathbf{x} - k^2 + C_0. \tag{2.7}$$

The corresponding SAV reformulated system leads to

$$\begin{cases} p_t = -\frac{1}{2\alpha}\Delta q - \frac{k}{\sqrt{\big(F(\phi,p,q),1\big)+C_0}}q\phi,\\ q_t = \frac{1}{2\alpha}\Delta p + \frac{k}{\sqrt{\big(F(\phi,p,q),1\big)+C_0}}p\phi,\\ \phi_t = \omega,\\ \omega_t = \Delta\phi - \beta^2\phi + \frac{k}{\sqrt{\big(F(\phi,p,q),1\big)+C_0}}(p^2+q^2),\\ k_t = \frac{1}{2\sqrt{\big(F(\phi,p,q),1\big)+C_0}}\big(\phi_t(p^2+q^2) + 2\phi(pp_t+qq_t),\,1\big), \end{cases} \tag{2.8}$$

with the consistent initial condition

$$(p,q,\phi,\omega)(\mathbf{x},0) = \big(\mathrm{Re}(\psi_0),\, \mathrm{Im}(\psi_0),\, \phi_0,\, \phi_1\big),\ k(0) = \sqrt{\big(F(\phi,\, p,\, q)|_{t=0},\, 1\big) + C_0} \quad \text{for } \mathbf{x}\in\bar{\Omega}.$$

Analogously, one can demonstrate the following mass and energy identities with slight modification of Theorem 2.1.

Theorem 2.2 *The SAV reformulated system* (2.8) *satisfies two conservation laws corresponding to the mass and energy defined in* (2.2) and (2.7)*, respectively.*

Proof It is similar to the proof of Theorem 2.1, so it is omitted. □

3 EQ-GRK schemes

In this section, we apply the GRK method as well as the Fourier pseudo-spectral method to discretize the above EQ reformulation system in time and space, respectively. The fully discrete schemes can reach arbitrarily high-order accuracy in time, which is compatible with the spectral order accuracy in space. It is worthwhile to note that these proposed schemes still conserve the corresponding mass and energy invariants at the discrete time level.

At the very beginning, we introduce some notations. For two positive even integers N_x and N_y, denote the spatial mesh sizes $h_x := (x_2 - x_1)/N_x$, $h_y := (y_2 - y_1)/N_y$ and the maximum length $h := \max\{h_x, h_y\}$. The time step is denoted as $\tau := T/N_t$ with N_t is also a positive integer. The discrete grid points are defined as $\Omega_h := \{\mathbf{x}_h = (x_1 + ih_x, y_1 + jh_y) | 1 \le i \le N_x, 1 \le j \le N_y\}$ and $\bar{\Omega}_h := \Omega_h \cup \partial\Omega$. Let $\mathbb{V}_h = \{v = (v_h), \mathbf{x}_h \in \bar{\Omega}_h\}$ be the space of gird functions. For any $u, v \in \mathbb{V}_h$, we define the discrete inner product $\langle u, v\rangle := h_x h_y \sum_{\mathbf{x}_h \in \Omega_h} u_h v_h$ and the associated l^2-norm $\|u\| := \sqrt{\langle u, u\rangle}$. Additionally, one also denote the discrete maximum norm $\|u\|_\infty = \max_{\mathbf{x}_h \in \Omega_h} |u_h|$ and the componentwise product of vectors $uv = (u_h v_h)$ with $\mathbf{x}_h \in \Omega_h$. Δ_f represents the Fourier pseudo-spectral approximation of Laplacian operator (see [37, Section 2] for details), and $\|\nabla_f u\| = \sqrt{\langle u, -\Delta_f u\rangle}$ for $u \in \mathbb{V}_h$.

With all above preparations, the fully discrete EQ-GRK schemes are presented as follows.

3.1 IEQ-GRK scheme

Scheme 3.1 *Let b_i, a_{ij} $(i, j = 1, \ldots, s)$ and $c_i = \sum_{j=1}^{s} a_{ij}$ be GRK coefficients. For given $\Upsilon^n \in \mathbb{V}_h$, where Υ is taken as P, Q, Φ, W and R, the following intermediate values are first calculated by*

$$\begin{cases} P_i^n = P^n + \tau \sum\limits_{j=1}^{s} a_{ij} \dot{P}_j^n, & \dot{P}_i^n = -\frac{1}{2\alpha}\Delta_f Q_i^n - \frac{R_i^n}{\mathcal{R}_i^n} Q_i^n \Phi_i^n, \\ Q_i^n = Q^n + \tau \sum\limits_{j=1}^{s} a_{ij} \dot{Q}_j^n, & \dot{Q}_i^n = \frac{1}{2\alpha}\Delta_f P_i^n + \frac{R_i^n}{\mathcal{R}_i^n} P_i^n \Phi_i^n, \\ \Phi_i^n = \Phi^n + \tau \sum\limits_{j=1}^{s} a_{ij} \dot{\Phi}_j^n, & \dot{\Phi}_i^n = W_i^n, \\ W_i^n = W^n + \tau \sum\limits_{j=1}^{s} a_{ij} \dot{W}_j^n, & \dot{W}_i^n = (\Delta_f - \beta^2)\Phi_i^n + \frac{R_i^n}{\mathcal{R}_i^n}\big((P_i^n)^2 + (Q_i^n)^2\big), \\ R_i^n = R^n + \tau \sum\limits_{j=1}^{s} a_{ij} \dot{R}_j^n, & \dot{R}_i^n = \frac{\dot{\Phi}_i^n\big((P_i^n)^2 + (Q_i^n)^2\big) + 2\Phi_i^n(P_i^n \dot{P}_i^n + Q_i^n \dot{Q}_i^n)}{2\mathcal{R}_i^n}, \end{cases} \tag{3.1}$$

where $\mathcal{R}_i^n := \sqrt{F(\Phi_i^n, P_i^n, Q_i^n) + C_0}$. Then, the numerical solutions Υ^{n+1} are updated by

$$\Upsilon^{n+1} = \Upsilon^n + \tau \sum_{i=1}^{s} b_i \dot{\Upsilon}_i^n. \tag{3.2}$$

3.2 SAV-GRK scheme

Scheme 3.2 *Let b_i, a_{ij} $(i, j = 1, \ldots, s)$ and $c_i = \sum_{j=1}^{s} a_{ij}$ be GRK coefficients. For given $\Upsilon^n \in \mathbb{V}_h$ and K^n, where Υ is taken as P, Q, Φ and W, the following intermediate values are first calculated by*

$$\begin{cases} P_i^n = P^n + \tau \sum\limits_{j=1}^{s} a_{ij} \dot{P}_j^n, & \dot{P}_i^n = -\frac{1}{2\alpha}\Delta_f Q_i^n - \frac{K_i^n}{\mathcal{K}^n} Q_i^n \Phi_i^n, \\ Q_i^n = Q^n + \tau \sum\limits_{j=1}^{s} a_{ij} \dot{Q}_j^n, & \dot{Q}_i^n = \frac{1}{2\alpha}\Delta_f P_i^n + \frac{K_i^n}{\mathcal{K}^n} P_i^n \Phi_i^n, \\ \Phi_i^n = \Phi^n + \tau \sum\limits_{j=1}^{s} a_{ij} \dot{\Phi}_j^n, & \dot{\Phi}_i^n = W_i^n, \\ W_i^n = W^n + \tau \sum\limits_{j=1}^{s} a_{ij} \dot{W}_j^n, & \dot{W}_i^n = (\Delta_f - \beta^2)\Phi_i^n + \frac{K_i^n}{\mathcal{K}^n}\big((P_i^n)^2 + (Q_i^n)^2\big), \\ K_i^n = K^n + \tau \sum\limits_{j=1}^{s} a_{ij} \dot{K}_j^n, & \dot{K}_i^n = \frac{\langle \dot{\Phi}_i^n, (P_i^n)^2 + (Q_i^n)^2 \rangle + 2\langle \Phi_i^n, P_i^n \dot{P}_i^n + Q_i^n \dot{Q}_i^n \rangle}{2\mathcal{K}^n}, \end{cases} \tag{3.3}$$

where $\mathcal{K}^n := \sqrt{\langle F(\Phi_i^n, P_i^n, Q_i^n), 1\rangle + C_0}$. Then, the numerical solutions Υ^{n+1} and K^{n+1} are updated by

$$\begin{cases} \Upsilon^{n+1} = \Upsilon^n + \tau \sum\limits_{i=1}^{s} b_i \dot{\Upsilon}_i^n, \\ K^{n+1} = K^n + \tau \sum\limits_{i=1}^{s} b_i \dot{K}_i^n. \end{cases} \tag{3.4}$$

The next two theorems indicate that the EQ-GRK schemes proposed above maintain the conservation properties of both mass and energy at the discrete time level.

Theorem 3.1 *The fully discrete IEQ-GRK scheme (3.1)–(3.2) are conservative in the sense that*

$$M^n = M^0 \quad \text{and} \quad E_{\text{ieq}}^n = E_{\text{ieq}}^0,$$

where

$$M^n = \|P^n\|^2 + \|Q^n\|^2,$$
$$E_{\text{ieq}}^n = \frac{1}{2}\Big(\frac{1}{\alpha}\|\nabla_f P^n\|^2 + \frac{1}{\alpha}\|\nabla_f Q^n\|^2 + \|\nabla_f \Phi^n\|^2 + \|W^n\|^2 + \beta^2\|\Phi^n\|^2\Big) - \|R^n\|^2 + C_0|\Omega|,$$

are the discrete mass and discrete energy, respectively.

Theorem 3.2 *The fully discrete SAV-GRK scheme (3.3)–(3.4) are conservative in the sense that*

$$M^n = M^0 \quad \text{and} \quad E_{\text{sav}}^n = E_{\text{sav}}^0,$$

where

$$\begin{aligned} M^n &= \|P^n\|^2 + \|Q^n\|^2, \\ E^n_{\text{sav}} &= \frac{1}{2}\left(\frac{1}{\alpha}\|\nabla_f P^n\|^2 + \frac{1}{\alpha}\|\nabla_f Q^n\|^2 + \|\nabla_f \Phi^n\|^2 + \|W^n\|^2 + \beta^2\|\Phi^n\|^2\right) \\ &\quad -(K^n)^2 + C_0, \end{aligned}$$

are the discrete mass and discrete energy, respectively.

We verify the assertion of SAV case in Theorem 3.2 and omit the proof of the IEQ case in Theorem 3.1 to save space. The latter could be borne out by modifying the former properly.

Proof Let $\Upsilon = P$ and taking the square of l^2-norm on both sides of the first relation of (3.4), it is not difficult to get

$$\|P^{n+1}\|^2 = \|P^n\|^2 + 2\tau\sum_{i=1}^{s} b_i\langle P^n, \dot{P}_i^n\rangle + \tau^2\sum_{i,j=1}^{s} b_i b_j\langle \dot{P}_i^n, \dot{P}_j^n\rangle.$$

Plugging the first relation of the first row of (3.3) into the second term on the right-hand side of the above equality, one has

$$\|P^{n+1}\|^2 = \|P^n\|^2 + 2\tau\sum_{i=1}^{s} b_i\langle P_i^n, \dot{P}_i^n\rangle - \tau^2\sum_{i,j=1}^{s} \varpi_{ij}\langle \dot{P}_i^n, \dot{P}_j^n\rangle,$$

where $\varpi_{ij} = b_i a_{ij} + b_j a_{ji} - b_i b_j$. The property of GRK coefficients yields $\varpi_{ij} = 0$ and

$$\|P^{n+1}\|^2 = \|P^n\|^2 + 2\tau\sum_{i=1}^{s} b_i\langle P_i^n, \dot{P}_i^n\rangle.$$

Analogously, it is straightforward to find

$$\|Q^{n+1}\|^2 = \|Q^n\|^2 + 2\tau\sum_{i=1}^{s} b_i\langle Q_i^n, \dot{Q}_i^n\rangle.$$

Adding both two equalities and then using the first two relations of the second column of (3.3), it reads that

$$\begin{aligned} M^{n+1} - M^n &= 2\tau\sum_{i=1}^{s} b_i\left[\langle P_i^n, \dot{P}_i^n\rangle + \langle Q_i^n, \dot{Q}_i^n\rangle\right] \\ &= 2\tau\sum_{i=1}^{s} b_i\left[\langle P_i^n, -\frac{1}{2\alpha}\Delta_f Q_i^n - \frac{K_i^n}{\mathcal{K}^n}Q_i^n\Phi_i^n\rangle + \langle Q_i^n, \frac{1}{2\alpha}\Delta_f P_i^n + \frac{K_i^n}{\mathcal{K}^n}P_i^n\Phi_i^n\rangle\right] \\ &= 0. \end{aligned} \tag{3.5}$$

This completes the proof of discrete mass conservation. Let $\Upsilon = P$ and the first relation of (3.4) implies that

$$-\Delta_f P^{n+1} = -\Delta_f P^n - \tau \sum_{i=1}^{s} b_i \Delta_f \dot{P}_i^n.$$

Taking the discrete inner product with P^{n+1}, one has

$$\begin{aligned}
\|\nabla_f P^{n+1}\|^2 &= \langle -\Delta_f P^n - \tau \sum_{i=1}^{s} b_i \Delta_f \dot{P}_i^n, P^n + \tau \sum_{i=1}^{s} b_i \dot{P}_i^n \rangle \\
&= \|\nabla_f P^n\| - 2\tau \sum_{i=1}^{s} b_i \langle \Delta_f P_i^n, \dot{P}_i^n \rangle + \tau^2 \sum_{i,j=1}^{s} \varpi_{ij} \langle \nabla_f \dot{P}_i^n, \nabla_f \dot{P}_j^n \rangle \\
&= \|\nabla_f P^n\| - 2\tau \sum_{i=1}^{s} b_i \langle \Delta_f P_i^n, \dot{P}_i^n \rangle,
\end{aligned}$$

where the first relation of the first row of (3.3) and the property of GRK coefficients were used. Similarly, one can obtain the following assertions

$$\begin{aligned}
&\|\nabla_f \Upsilon^{n+1}\|^2 = \|\nabla_f \Upsilon^n\|^2 - 2\tau \sum_{i=1}^{s} b_i \langle \Delta_f \Upsilon_i^n, \dot{\Upsilon}_i^n \rangle \quad \text{for } \Upsilon = Q \text{ and } \Phi, \\
&\|\Upsilon^{n+1}\|^2 = \|\Upsilon^n\|^2 + 2\tau \sum_{i=1}^{s} b_i \langle \Upsilon_i^n, \dot{\Upsilon}_i^n \rangle \quad \text{for } \Upsilon = W \text{ and } \Phi, \\
&(K^{n+1})^2 = (K^n)^2 + 2\tau \sum_{i=1}^{s} b_i K_i^n \dot{K}_i^n.
\end{aligned}$$

From the definition of discrete energy in Theorem 3.2, we add the aforementioned results and possess

$$\begin{aligned}
E_{\text{sav}}^{n+1} - E_{\text{sav}}^n = -\tau \sum_{i=1}^{s} b_i \big[&\frac{1}{\alpha} \langle \Delta_f P_i^n, \dot{P}_i^n \rangle + \frac{1}{\alpha} \langle \Delta_f Q_i^n, \dot{Q}_i^n \rangle + \langle \Delta_f \Phi_i^n, \dot{\Phi}_i^n \rangle - \langle W_i^n, \dot{W}_i^n \rangle \\
&- \beta^2 \langle \Phi_i^n, \dot{\Phi}_i^n \rangle + 2 K_i^n \dot{K}_i^n \big].
\end{aligned}$$

Substituting the second column of (3.3) into the right-hand side of the above equality, it arrives at the final result and complete the proof of Theorem 3.2. □

Remark 1 The EQ reformulation offers an elegant platform for developing structure-preserving high-order schemes. The number of GRK coefficients (Gaussian quadrature nodes) $c_1, c_2, \ldots, c_s$ actually determines the temporal accuracy. In [20], the authors validated that the GRK method has the same order $2s$ as the relevant Gaussian quadrature formula, which results in the arbitrarily high-order accuracy in time for the proposed algorithms.

It is obvious that the suggested EQ-GRK schemes are coupled and implicit, which requires nonlinear iteration at each time level. For the IEQ-GRK scheme, in practical computation, we often set

$$P_i^n = P^n, \quad Q_i^n = Q^n, \quad \Phi_i^n = \Phi^n, \quad R_i^n = R^n$$

to treat the nonlinear part of (3.1) explicitly. Based on the iterative errors of P_i^n, Q_i^n and Φ_i^n, (3.1) is carried out efficiently to calculate the values of $\dot{\Upsilon}_i^n$ ($\Upsilon = P, Q, \Phi, W, R$). We then get the numerical solutions on the next time layer via (3.2) and update the iterative values. For the other scheme (**Scheme 3.2**), however, we only set

$$P_i^n = P^n, \quad Q_i^n = Q^n, \quad \Phi_i^n = \Phi^n$$

for the nonlinear part of (3.3). The discrete inner products of $\dot{K}_i^n$ are calculated systematically by solving the corresponding linear equations in (3.3), and the values of $\dot{\Upsilon}_i^n$ ($\Upsilon = P, Q, \Phi, W, K$) are obtained invoking to the iterative errors of P_i^n, Q_i^n and Φ_i^n (see Appendix for details). We then get the numerical solutions and update the iterative values in the same spirit.

4 EQ-GRK-PC schemes

In order to reduce the computational cost and improve the accuracy as well as the stability, in this section, we employ the prediction-correction technique and design another class of conservative algorithms named EQ-GRK-PC scheme for the EQ reformulated system.

4.1 IEQ-GRK-PC scheme

Scheme 4.1 *Let b_i, a_{ij} $(i, j = 1, \ldots, s)$ and $c_i = \sum_{j=1}^s a_{ij}$ be GRK coefficients. For given $\Upsilon^n \in \mathbb{V}_h$, where Υ is taken as P, Q, Φ, W and R, the intermediate values are first calculated by the following prediction-correction technique*

Prediction: *Denote λ and Λ are iteration variable and iteration step, respectively. One set $\Upsilon_i^{n(0)} = \Upsilon^n$, then compute $\Upsilon_i^{n(\lambda+1)}$, $\dot{\Upsilon}_i^{n(\lambda+1)}$ ($\Upsilon = P, Q, \Phi, W$) and $\dot{R}_i^{n(\lambda+1)}$, $R_i^{n(\lambda+1)}$ sequentially from $\lambda = 0$ to Λ via*

$$\begin{cases}
P_i^{n(\lambda+1)} = P^n + \tau \sum\limits_{j=1}^s a_{ij} \dot{P}_j^{n(\lambda+1)}, & \dot{P}_i^{n(\lambda+1)} = -\frac{1}{2\alpha} \Delta_f Q_i^{n(\lambda+1)} - \frac{R_i^{n(\lambda)}}{\mathcal{R}_i^{n(\lambda)}} Q_i^{n(\lambda)} \Phi_i^{n(\lambda)}, \\
Q_i^{n(\lambda+1)} = Q^n + \tau \sum\limits_{j=1}^s a_{ij} \dot{Q}_j^{n(\lambda+1)}, & \dot{Q}_i^{n(\lambda+1)} = \frac{1}{2\alpha} \Delta_f P_i^{n(\lambda+1)} + \frac{R_i^{n(\lambda)}}{\mathcal{R}_i^{n(\lambda)}} P_i^{n(\lambda)} \Phi_i^{n(\lambda)}, \\
\Phi_i^{n(\lambda+1)} = \Phi^n + \tau \sum\limits_{j=1}^s a_{ij} \dot{\Phi}_j^{n(\lambda+1)}, & \dot{\Phi}_i^{n(\lambda+1)} = W_i^{n(\lambda+1)}, \\
W_i^{n(\lambda+1)} = W^n + \tau \sum\limits_{j=1}^s a_{ij} \dot{W}_j^{n(\lambda+1)}, & \dot{W}_i^{n(\lambda+1)} = (\Delta_f - \beta^2) \Phi_i^{n(\lambda+1)} + \frac{R_i^{n(\lambda)}}{\mathcal{R}_i^{n(\lambda)}} \big((P_i^{n(\lambda)})^2 + (Q_i^{n(\lambda)})^2 \big), \\
\dot{R}_i^{n(\lambda+1)} = \frac{\dot{\Phi}_i^{n(\lambda+1)} \big((P_i^{n(\lambda+1)})^2 + (Q_i^{n(\lambda+1)})^2 \big) + 2\Phi_i^{n(\lambda+1)} \big(P_i^{n(\lambda+1)} \dot{P}_i^{n(\lambda+1)} + Q_i^{n(\lambda+1)} \dot{Q}_i^{n(\lambda+1)} \big)}{2\mathcal{R}_i^{n(\lambda+1)}}, \\
R_i^{n(\lambda+1)} = R^n + \tau \sum\limits_{j=1}^s a_{ij} \dot{R}_j^{n(\lambda+1)}.
\end{cases}$$

For a given tolerance error $TOL > 0$, if

$$\max_{1\le i\le s} \|\Upsilon_i^{n(\lambda+1)} - \Upsilon_i^{n(\lambda)}\|_\infty < TOL \quad \text{for } \Upsilon = P, Q \text{ and } \Phi,$$

we stop the iteration and set $\Upsilon_i^{n,*} = \Upsilon_i^{n(\lambda+1)}$ ($\Upsilon = P, Q, \Phi, R$); otherwise, one set $\Upsilon_i^{n,*} = \Upsilon_i^{n(\Lambda)}$.

Correction: *For the predicted $\Upsilon_i^{n,*}$ ($\Upsilon = P, Q, \Phi, R$), we calculate the intermediate values by*

$$\begin{cases} P_i^n = P^n + \tau \sum\limits_{j=1}^{s} a_{ij}\dot{P}_j^n, & \dot{P}_i^n = -\frac{1}{2\alpha}\Delta_f Q_i^n - \frac{R_i^{n,*}}{\mathcal{R}_i^{n,*}} Q_i^{n,*}\Phi_i^{n,*}, \\ Q_i^n = Q^n + \tau \sum\limits_{j=1}^{s} a_{ij}\dot{Q}_j^n, & \dot{Q}_i^n = \frac{1}{2\alpha}\Delta_f P_i^n + \frac{R_i^{n,*}}{\mathcal{R}_i^{n,*}} P_i^{n,*}\Phi_i^{n,*}, \\ \Phi_i^n = \Phi^n + \tau \sum\limits_{j=1}^{s} a_{ij}\dot{\Phi}_j^n, & \dot{\Phi}_i^n = W_i^n, \\ W_i^n = W^n + \tau \sum\limits_{j=1}^{s} a_{ij}\dot{W}_j^n, & \dot{W}_i^n = (\Delta_f - \beta^2)\Phi_i^n + \frac{R_i^{n,*}}{\mathcal{R}_i^{n,*}}\big((P_i^{n,*})^2 + (Q_i^{n,*})^2\big), \\ \dot{R}_i^n = \frac{\dot{\Phi}_i^n\left((P_i^{n,*})^2+(Q_i^{n,*})^2\right)+2\Phi_i^{n,*}(P_i^{n,*}\dot{P}_i^n+Q_i^{n,*}\dot{Q}_i^n)}{2\mathcal{R}_i^{n,*}}. \end{cases}$$

Then, the numerical solutions Υ^{n+1} ($\Upsilon = P, Q, \Phi, W, R$) are updated by

$$\Upsilon^{n+1} = \Upsilon^n + \tau \sum_{i=1}^{s} b_i \dot{\Upsilon}_i^n.$$

4.2 SAV-GRK-PC scheme

Scheme 4.2 *Let b_i, a_{ij} $(i, j = 1, \ldots, s)$ and $c_i = \sum_{j=1}^{s} a_{ij}$ be GRK coefficients. For given $\Upsilon^n \in \mathbb{V}_h$ and K^n, where Υ is taken as P, Q, Φ and W, the intermediate values are first calculated by the following prediction-correction technique*

Prediction: *Denote λ and Λ are iteration variable and iteration step, respectively. One set $\Upsilon_i^{n(0)} = \Upsilon^n$ and $K_i^{n(0)} = K^n$, then compute $\Upsilon_i^{n(\lambda+1)}$, $\dot{\Upsilon}_i^{n(\lambda+1)}$ and $\dot{K}_i^{n(\lambda+1)}$, $K_i^{n(\lambda+1)}$ sequentially from $\lambda = 0$ to Λ via*

$$\begin{cases} P_i^{n(\lambda+1)} = P^n + \tau \sum\limits_{j=1}^{s} a_{ij}\dot{P}_j^{n(\lambda+1)}, & \dot{P}_i^{n(\lambda+1)} = -\frac{1}{2\alpha}\Delta_f Q_i^{n(\lambda+1)} - \frac{K_i^{n(\lambda)}}{\mathcal{K}^{n(\lambda)}} Q_i^{n(\lambda)}\Phi_i^{n(\lambda)}, \\ Q_i^{n(\lambda+1)} = Q^n + \tau \sum\limits_{j=1}^{s} a_{ij}\dot{Q}_j^{n(\lambda+1)}, & \dot{Q}_i^{n(\lambda+1)} = \frac{1}{2\alpha}\Delta_f P_i^{n(\lambda+1)} + \frac{K_i^{n(\lambda)}}{\mathcal{K}^{n(\lambda)}} P_i^{n(\lambda)}\Phi_i^{n(\lambda)}, \\ \Phi_i^{n(\lambda+1)} = \Phi^n + \tau \sum\limits_{j=1}^{s} a_{ij}\dot{\Phi}_j^{n(\lambda+1)}, & \dot{\Phi}_i^{n(\lambda+1)} = W_i^{n(\lambda+1)}, \\ W_i^{n(\lambda+1)} = W^n + \tau \sum\limits_{j=1}^{s} a_{ij}\dot{W}_j^{n(\lambda+1)}, & \dot{W}_i^{n(\lambda+1)} = (\Delta_f - \beta^2)\Phi_i^{n(\lambda+1)} + \frac{K_i^{n(\lambda)}}{\mathcal{K}^{n(\lambda)}}\big((P_i^{n(\lambda)})^2 + (Q_i^{n(\lambda)})^2\big), \\ \dot{K}_i^{n(\lambda+1)} = \frac{\langle\dot{\Phi}_i^{n(\lambda+1)},(P_i^{n(\lambda+1)})^2+(Q_i^{n(\lambda+1)})^2\rangle+2\langle\Phi_i^{n(\lambda+1)},P_i^{n(\lambda+1)}\dot{P}_i^{n(\lambda+1)}+Q_i^{n(\lambda+1)}\dot{Q}_i^{n(\lambda+1)}\rangle}{2\mathcal{K}^{n(\lambda+1)}}, \\ K_i^{n(\lambda+1)} = K^n + \tau \sum\limits_{j=1}^{s} a_{ij}\dot{K}_j^{n(\lambda+1)}. \end{cases}$$

For a given tolerance error $TOL > 0$, if

$$\max_{1\le i\le s} \|\Upsilon_i^{n(\lambda+1)} - \Upsilon_i^{n(\lambda)}\|_\infty < TOL \quad \text{for } \Upsilon = P, Q \text{ and } \Phi,$$

we stop the iteration and set $\Upsilon_i^{n,*} = \Upsilon_i^{n(\lambda+1)}$; otherwise, one set $\Upsilon_i^{n,*} = \Upsilon_i^{n(\Lambda)}$.

Correction: *For the predicted $\Upsilon_i^{n,*}$ ($\Upsilon = P, Q, \Phi$), we calculate the intermediate values by*

$$\begin{cases} P_i^n = P^n + \tau \sum_{j=1}^{s} a_{ij}\dot{P}_j^n, & \dot{P}_i^n = -\frac{1}{2\alpha}\Delta_f Q_i^n - \frac{K_i^n}{\mathcal{K}^{n,*}} Q_i^{n,*}\Phi_i^{n,*}, \\ Q_i^n = Q^n + \tau \sum_{j=1}^{s} a_{ij}\dot{Q}_j^n, & \dot{Q}_i^n = \frac{1}{2\alpha}\Delta_f P_i^n + \frac{K_i^n}{\mathcal{K}^{n,*}} P_i^{n,*}\Phi_i^{n,*}, \\ \Phi_i^n = \Phi^n + \tau \sum_{j=1}^{s} a_{ij}\dot{\Phi}_j^n, & \dot{\Phi}_i^n = W_i^n, \\ W_i^n = W^n + \tau \sum_{j=1}^{s} a_{ij}\dot{W}_j^n, & \dot{W}_i^n = (\Delta_f - \beta^2)\Phi_i^n + \frac{K_i^n}{\mathcal{K}^{n,*}}\big((P_i^{n,*})^2 + (Q_i^{n,*})^2\big), \\ K_i^n = K^n + \tau \sum_{j=1}^{s} a_{ij}\dot{K}_j^n, & \dot{K}_i^n = \frac{\langle \dot{\Phi}_i^n, (P_i^{n,*})^2 + (Q_i^{n,*})^2\rangle + 2\langle \Phi_i^{n,*}, P_i^{n,*}\dot{P}_i^n + Q_i^{n,*}\dot{Q}_i^n\rangle}{2\mathcal{K}^{n,*}}. \end{cases}$$

Then, the numerical solutions Υ^{n+1} ($\Upsilon = P, Q, \Phi, W$) and K^{n+1} are updated by

$$\begin{cases} \Upsilon^{n+1} = \Upsilon^n + \tau \sum_{i=1}^{s} b_i \dot{\Upsilon}_i^n, \\ K^{n+1} = K^n + \tau \sum_{i=1}^{s} b_i \dot{K}_i^n. \end{cases}$$

Different from the previous nonlinear EQ-GRK schemes, the PC procedures mentioned above are linearized and decoupled. The prediction process of **Scheme 4.1** is displayed as

$$\Upsilon^n, \Upsilon_i^{n(0)}(\Upsilon = P, Q, \Phi, W, R) \Rightarrow \Upsilon_i^{n(1)}, \dot{\Upsilon}_i^{n(1)}(\Upsilon = P, Q, \Phi, W) \Rightarrow \dot{R}_i^{n(1)} \Rightarrow R_i^{n(1)}$$
$$\Rightarrow \Upsilon^n, \Upsilon_i^{n(1)}(\Upsilon = P, Q, \Phi, W, R) \Rightarrow \cdots \Rightarrow \Upsilon_i^{n,*}(\Upsilon = P, Q, \Phi, R).$$

According to the values of $\Upsilon_i^{n,*}$, the correction procedure is coincide with the one-step IEQ-GRK scheme. Similarly, the prediction implementation of SAV-GRK-PC scheme could be done with slight modification of the IEQ case, and the correction process is same to the one-step SAV-GRK scheme. It should be noticed that one can use fast Fourier transform (FFT) to solve the linear algebraic systems at each time step efficiently to speed up the practical computation.

Furthermore, we demonstrate that the EQ-GRK-PC schemes preserve the following energy conservation laws.

Theorem 4.1 *The fully discrete IEQ-GRK-PC scheme and the fully discrete SAV-GRK-PC scheme satisfy the energy invariants*

$$E_{\text{ieq}}^n = E_{\text{ieq}}^0 \quad \textit{and} \quad E_{\text{sav}}^n = E_{\text{sav}}^0,$$

where two discrete energies are defined in Theorems 3.1 and 3.2, respectively.

Proof Invoking to the correction procedure and the proof of Theorem 3.2 one can verify the discrete energy property of SAV-GRK-PC scheme. The other case can be proved similarly. □

Remark 2 From the first two relations of the second column of **Correction** in **Scheme 4.2**, it is readily to check that (3.5) is no longer available. This means the discrete mass conservation is absent in the proposed EQ-GRK-PC schemes, which would be tested in numerical examples.

Remark 3 The energy of EQ method, in fact, is the modified energy, instead of the original one. It is obvious that the former is equivalent to the latter in the continuous case, but not in the discrete case due to the truncation errors. Zhang et al. [38] demonstrate that the modified and original laws are equivalent numerically for the Cahn-Hilliard equation under certain constrains. Furthermore, by introducing an essential relaxation technique, Zhao et al. [39, 40] present some remedies to improve the accuracy and consistency of EQ method.

5 Numerical experiments

Three numerical examples are presented to verify the practicability, accuracy and conservation laws of the suggested algorithms in this section. In what follows, we choose the EQ parameter $C_0 = 2$ and set the tolerance error TOL = 1e-14 in prediction and iteration procedures without further declaration.

In order to quantify the numerical results, we define the solution errors of ψ and ϕ as $e_1(\tau, h) = \|\Psi^{N_t} - \psi(t_{N_t})\|_\infty$ ($\Psi = P + \mathrm{i}Q$) and $e_2(\tau, h) = \|\Phi^{N_t} - \phi(t_{N_t})\|_\infty$, respectively. The corresponding experimental rates in time are calculated by

$$\text{Order} \approx \log_2\left(e_\nu(\tau, h_0)/e_\nu(\tau/2, h_0)\right) \quad \text{for } \nu = 1, 2.$$

In addition, one also denote the relative errors of invariants in discrete nth time level as

$$RM^n = \frac{|M^n - M^0|}{M^0}, \quad RE_{\text{ieq}}^n = \frac{|E_{\text{ieq}}^n - E_{\text{ieq}}^0|}{E_{\text{ieq}}^0}, \quad RE_{\text{sav}}^n = \frac{|E_{\text{sav}}^n - E_{\text{sav}}^0|}{E_{\text{sav}}^0} \quad \text{for } n = 1, 2, \ldots, N_t.$$

Example 1 We consider the KGS equation on the region $[0, 2\pi] \times [0, 2\pi]$ with the parameters $\alpha = 2$ and $\beta = 1$. It has the following analytic solutions

$$\psi(x, y, t) = \exp\left(\mathrm{i}(x + y + 0.5t)\right), \quad \phi(x, y, t) = |\psi(x, y, t)|.$$

Table 1 Spatial errors of various GRK schemes at $T = 1$ with τ_0 = 1e-05

	IEQ-GRK		SAV-GRK		IEQ-GRK-PC($\Lambda = 3$)		SAV-GRK-PC($\Lambda = 3$)	
h	$e_1(\tau_0, h)$	$e_2(\tau_0, h)$	$e_1(\tau_0, h)$	$e_2(\tau_0, h)$	$e_1(\tau_0, h)$	$e_2(\tau_0, h)$	$e_1(\tau_0, h)$	$e_2(\tau_0, h)$
$\pi/4$	2.42e-14	1.11e-16	2.77e-14	1.11e-16	2.42e-14	1.11e-16	2.76e-14	1.11e-16
$\pi/8$	1.76e-14	1.11e-16	1.90e-14	1.11e-16	1.63e-14	1.11e-16	1.87e-14	1.11e-16

We employ the 2-stage GRK method with the RK coefficients

$$\begin{array}{c|cc} \frac{1}{2}-\frac{\sqrt{3}}{6} & \frac{1}{4} & \frac{1}{4}-\frac{\sqrt{3}}{6} \\ \frac{1}{2}+\frac{\sqrt{3}}{6} & \frac{1}{4}+\frac{\sqrt{3}}{6} & \frac{1}{4} \\ \hline & \frac{1}{2} & \frac{1}{2} \end{array}$$

to verify the convergence orders of the schemes mentioned above. The spatial accuracy is tested with the halving space lengths by fixing a sufficiently small τ_0 = 1e-05 to avoid contamination of the temporal error. Solution errors listed in Table 1 show the spatial errors are almost negligible, which confirms that the Fourier pseudo-spectral method is of arbitrary order of accuracy for the sufficiently smooth or analytic problem.

The temporal errors and orders are then examined on the halving time steps with the space size $h_0 = \pi/64$. For the PC schemes, we here choose the iteration step $\Lambda = 3$ in the prediction procedure. Numerical results in Fig. 1 state clearly that all the proposed schemes have fourth-order accuracy in time. It is highly in coincidence with the theoretical explanation in Remark 1. To further study the PC technique, one also depict the temporal convergence orders of EQ-GRK-PC schemes in Fig. 2 with different iteration steps. Observation from Fig. 2 indicates that a one-step prediction calculation improve the accuracy by one order for both IEQ and SAV cases. Combined with the relevant results in Fig. 1, one can conclude that, by incorporating the above PC schemes, only three prediction steps are needed to achieve fourth-order

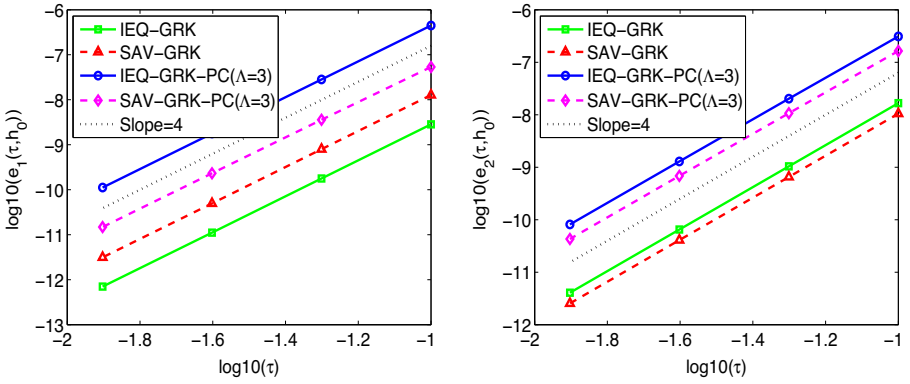

Fig. 1 Temporal convergence orders of various GRK schemes with $h_0 = \pi/64$ at $T = 1$

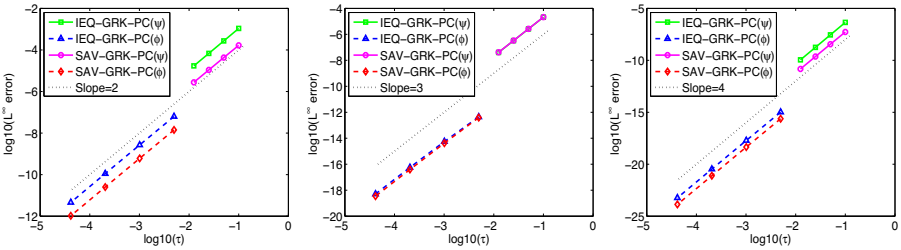

(a) $\Lambda = 1$ (b) $\Lambda = 2$ (c) $\Lambda = 3$

Fig. 2 Temporal convergence orders of EQ-GRK-PC schemes with different Λ at $T = 1$

accuracy. Moreover, we consider the same solution errors of EQ-GRK schemes and EQ-GRK-PC schemes, and then record the minimum iteration steps and CPU time of various GRK schemes in Table 2 for comparison. From the left column of Table 2, we observe that the iteration steps of the nonlinear EQ-GRK schemes decrease as the time step is halved, no matter for IEQ case or SAV case. Compared with the results on the right column, it is readily to find that the EQ-GRK-PC schemes can obtain almost the same errors with fewer iterations and CPU time under the same conditions. This again witnesses the power and great performance of PC strategy.

Example 2 We take another KGS example in 2D with the parameters $\alpha = 1/2$ and $\beta = 1$ to investigate the conservation laws and the evolution of solutions [15]. The computational domain is chosen as $\Omega = [-32, 32] \times [-32, 32]$ and the initial conditions are taken as

$$\psi_0(x, y) = \frac{2}{\exp(x^2+2y^2)+\exp(-x^2-2y^2)} \exp\left(\frac{5\,\mathrm{i}}{\cosh(\sqrt{4x^2+y^2})}\right),$$
$$\phi_0(x, y) = \exp(-x^2 - y^2), \quad \phi_1(x, y) = \tfrac{1}{2}\exp(-x^2 - y^2).$$

On the one hand, we choose the time step $\tau = 1/50$ and the space size $h = 1/4$ to simulate the discrete conservation laws of various GRK schemes at $T = 20$.

Table 2 Minimum iteration steps of various GRK schemes with $h_0 = \pi/64$ at $T = 1$

τ	$e_1(\tau, h_0)$	$e_2(\tau, h_0)$	Step	CPU(s)	$e_1(\tau, h_0)$	$e_2(\tau, h_0)$	Λ	CPU(s)
	IEQ-GRK				IEQ-GRK-PC			
1/10	2.84e-09	1.66e-08	10	0.57	3.20e-09	1.69e-08	5	0.33
1/20	1.78e-10	1.04e-09	8	0.71	1.83e-10	1.04e-09	5	0.54
1/40	1.11e-11	6.49e-11	7	1.17	1.12e-11	6.50e-11	5	1.03
	SAV-GRK				SAV-GRK-PC			
1/10	1.27e-08	1.05e-08	8	0.86	1.33e-08	9.99e-09	4	0.37
1/20	7.94e-10	6.54e-10	7	1.30	8.04e-10	6.46e-10	4	0.61
1/40	4.96e-11	4.09e-11	6	2.18	4.98e-11	4.07e-11	4	1.11

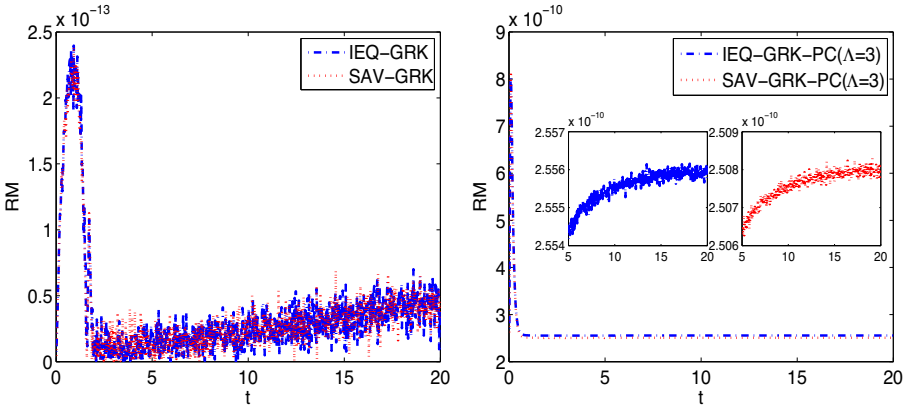

Fig. 3 Relative mass errors of EQ-GRK schemes (left) and EQ-GRK-PC schemes (right) with $\tau = 1/50$ and $h = 1/4$ at $T = 20$

Figure 3 shows the relative mass errors of presented schemes and experimental results witness the theoretical analysis, i.e., the nonlinear EQ-GRK schemes can preserve the discrete mass invariant well whereas the EQ-GRK-PC schemes can not. From Fig. 4, we evidently observe that the relative errors of modified energy in different scenarios are all conserved up to round-off error during a long period of time. This indicates that two classes of GRK schemes inherit the discrete energy conservation laws which are agreement with the continuous cases in Theorems 2.1 and 2.2. Error comparison of two subfigures in Fig. 4 reveals that the SAV strategy may be more suitable than the IEQ one in satisfying the energy conservation.

On the other hand, the evolution of two solutions are investigated with the same time step $\tau = 1/50$ and the space size $h = 1/4$. Figure 5 shows the surface plots of nucleon density $|\psi|^2$ and meson field ϕ by utilizing the 2-stage IEQ-GRK scheme.

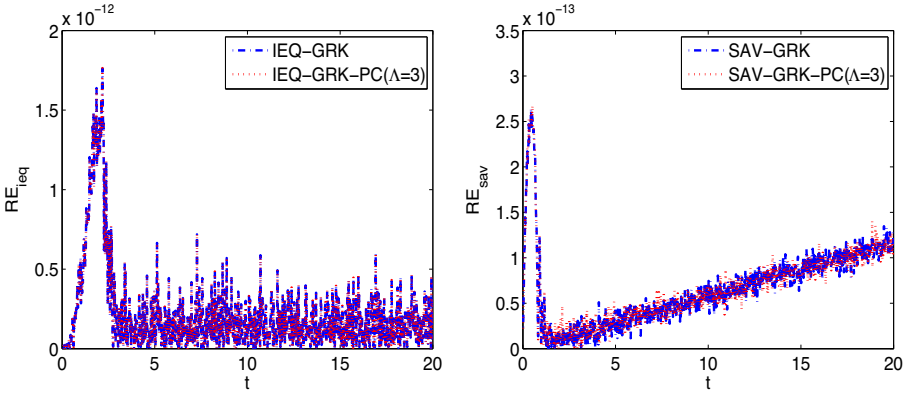

Fig. 4 Relative modified energy errors of IEQ-GRK schemes (left) and SAV-GRK schemes (right) with $\tau = 1/50$ and $h = 1/4$ at $T = 20$

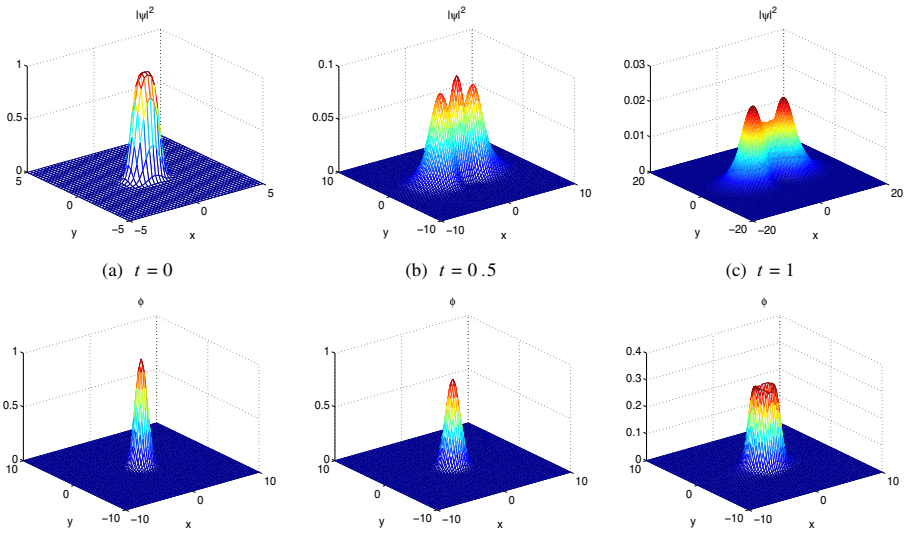

(a) $t = 0$ (b) $t = 0.5$ (c) $t = 1$

Fig. 5 The evolution of $|\psi|^2$ (upper) and ϕ (lower) at different times with $\tau = 1/50$ and $h = 1/4$ using the 2-stage IEQ-GRK scheme

They are in good agreement with the results in previous studies, for instance [15, 16]. Numerical behaviors of other three GRK schemes are tested subsequently and the same conclusion can be drawn. We omit it here to save space. The concerned results demonstrate the validity and capability of the proposed methods.

Example 3 Last but not the least, we investigate the dynamics of waves in the 2D KGS system with the parameters $\alpha = \beta = 1$ under a general initial localized data [10]

$$\psi_0(x, y) = (1 + \mathrm{i})e^{-(x^2+y^2)}, \quad \phi_0(x, y) = \mathrm{sech}(x^2 + y^2), \quad \phi_1(x, y) = \sin(x + y)e^{-2(x^2+y^2)}.$$

The computational domain is taken as $\Omega = [-10, 10] \times [-10, 10]$.

Always, we apply the above GRK method to address this issue. The 3-stage SAV-GRK-PC method with the RK coefficients

$$\begin{array}{c|ccc} \frac{1}{2} - \frac{\sqrt{15}}{10} & \frac{5}{36} & \frac{2}{9} - \frac{\sqrt{15}}{15} & \frac{5}{36} - \frac{\sqrt{15}}{30} \\ \frac{1}{2} & \frac{5}{36} + \frac{\sqrt{15}}{24} & \frac{2}{9} & \frac{5}{36} - \frac{\sqrt{15}}{24} \\ \frac{1}{2} + \frac{\sqrt{15}}{10} & \frac{5}{36} + \frac{\sqrt{15}}{30} & \frac{2}{9} + \frac{\sqrt{15}}{15} & \frac{5}{36} \\ \hline & \frac{5}{18} & \frac{4}{9} & \frac{5}{18} \end{array}$$

is employed to exhibit the generality of the s-stage GRK methods. We choose $T = 1$ and carry out the time step refinement test from $\tau = 1/20$ to $1/320$ with a fixed

Table 3 Temporal errors and orders of 3-stage SAV-GRK-PC scheme with $h_0 = 1/40$ at $T = 1$

τ	1/20	1/40	1/80	1/160	1/320
$e_1(\tau_0, h)$	—	5.46e-07	1.83e-08	3.54e-10	5.79e-12
Order		*	4.91	5.70	5.93
$e_2(\tau_0, h)$	—	4.92e-09	7.73e-11	1.21e-12	1.93e-14
Order		*	5.99	6.00	5.97

spacing size $h_0 = 1/40$. The corresponding errors and orders are tabulated in Table 3. As can be seen, it is of sixth-order accurate which again confirms the effectiveness of GRK method. Subsequently, we take $\tau = h = 1/20$ to simulate the dynamics of waves and plot the evolution of two solutions $|\psi|$ and ϕ in Fig. 6. Compared with the parameters in earlier work, new strategies in this work can be implemented in a relative large time step (about a five-fold increase). Analogously, one can adopt large step size and other 3-stage GRK methods presented above to obtain the same results which are omitted here for simplicity. All these results indicate that the s-stage GRK methods are feasible and the aforementioned methods are effective in dealing with the KGS equation numerically.

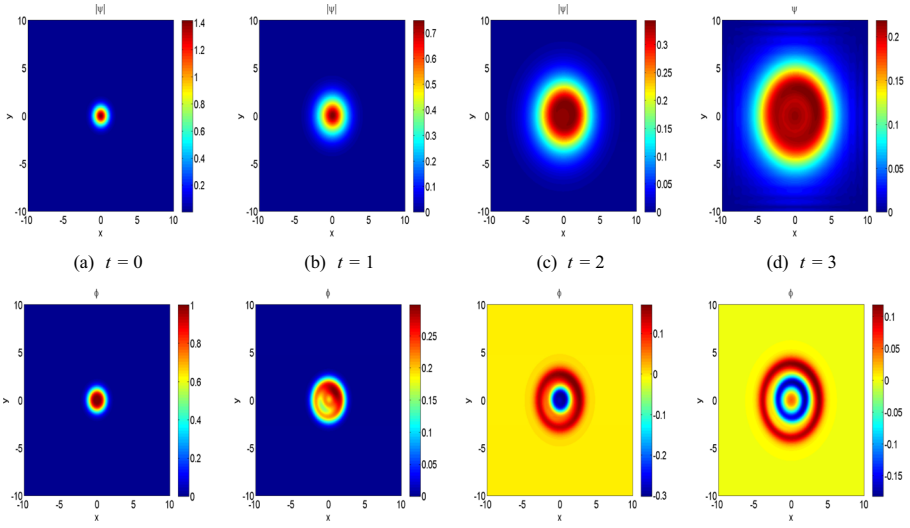

Fig. 6 Aerial views of $|\psi|$ (left) and ϕ (right) at different times with $\tau = h = 1/20$ using the 3-stage SAV-GRK-PC scheme

6 Conclusion

By introducing the EQ approach and the PC technique, we apply the s-stage GRK method as well as the Fourier pseudo-spectral method to develop two classes of fully discrete numerical schemes for solving the KGS equation. These schemes maintain the invariants in discrete sense and can reach high-order accuracy in both time and space. Numerical results and comparisons are displayed to illustrate the superior performance. We point out that the suggested methods can also be generalized to other conservative systems. The EQ method respects a modified energy law according to the auxiliary variables rather than the original variables. Truncation errors are introduced during numerical computations so that the numerical solutions of the auxiliary variables are no longer equivalent to their original continuous definitions. The authors in [41] and [42] present the Lagrange multiplier method and the supplementary variable method, respectively, to fill this gap. Unfortunately, the temporal accuracy is second-order and the development of high-order schemes is still open. This needs to be further studied in our next work.

Appendix A

We take 2-stage GRK method as an example to illustrate the process of **Scheme 3.2** in detail. For the iterative values P_i^n, Q_i^n and Φ_i^n $(i = 1, 2)$, we first denote

$$X_i^n := \frac{(P_i^n)^2 + (Q_i^n)^2}{\mathcal{K}^n}, \quad Y_i^n := \frac{P_i^n \Phi_i^n}{\mathcal{K}^n}, \quad Z_i^n := \frac{Q_i^n \Phi_i^n}{\mathcal{K}^n}.$$

Then, from the last three rows of (3.3), one has

$$\begin{aligned} \dot{K}_i^n &= \frac{\langle \dot{\Phi}_i^n, (P_i^n)^2 + (Q_i^n)^2 \rangle}{2\mathcal{K}^n} + \frac{\langle \dot{P}_i^n, P_i^n \Phi_i^n \rangle}{\mathcal{K}^n} + \frac{\langle \dot{Q}_i^n, Q_i^n \Phi_i^n \rangle}{\mathcal{K}^n} \\ &= \frac{1}{2}\langle \dot{\Phi}_i^n, X_i^n \rangle + \langle \dot{P}_i^n, Y_i^n \rangle + \langle \dot{Q}_i^n, Z_i^n \rangle \triangleq \mathrm{I}_i^n + \mathrm{II}_i^n + \mathrm{III}_i^n, \end{aligned}$$

and

$$\begin{aligned} \dot{\Phi}_i^n &= W^n + \tau \sum_{j=1}^{2} a_{ij} \big[(\Delta_f - \beta^2)\Phi_j^n + K_j^n X_j^n \big] \\ &= W^n + \tau \sum_{j=1}^{2} a_{ij} \big[(\Delta_f - \beta^2)(\Phi^n + \tau \sum_{\ell=1}^{2} a_{j\ell} \dot{\Phi}_\ell^n) + (K^n + \tau \sum_{\ell=1}^{2} a_{j\ell} \dot{K}_\ell^n) X_j^n \big]. \end{aligned}$$

The above equality is rewritten explicitly and it yields

$$\begin{aligned} \mathcal{A}\dot{\Phi}_1^n + \mathcal{B}\dot{\Phi}_2^n &= \Gamma_1^n + \tau^2 (a_{11}^2 X_1^n + a_{12}a_{21} X_2^n)\dot{K}_1^n + \tau^2 (a_{11}a_{12} X_1^n + a_{12}a_{22} X_2^n)\dot{K}_2^n, \\ \mathcal{C}\dot{\Phi}_1^n + \mathcal{A}\dot{\Phi}_2^n &= \Gamma_2^n + \tau^2 (a_{21}a_{11} X_1^n + a_{22}a_{21} X_2^n)\dot{K}_1^n + \tau^2 (a_{21}a_{12} X_1^n + a_{22}^2 X_2^n)\dot{K}_2^n, \end{aligned}$$

where

$$\mathcal{A} = 1-\tau^2(a_{11}^2+a_{12}a_{21})(\Delta_f-\beta^2),\ \ \mathcal{B} = -2\tau^2 a_{11}a_{12}(\Delta_f-\beta^2),\ \ \mathcal{C} = -2\tau^2 a_{11}a_{21}(\Delta_f-\beta^2),$$
$$\Gamma_i^n = W^n+\tau(a_{i1}+a_{i2})(\Delta_f-\beta^2)\Phi^n+\tau(a_{i1}X_1^n+a_{i2}X_2^n)K^n,$$

and the coefficient property of 2-stage GRK method $a_{11} = a_{22}$ was used. Some simple calculations imply that

$$\dot{\Phi}_i^n = A_i^n + B_i^n\dot{K}_1^n + C_i^n\dot{K}_2^n \quad \text{for } i=1,2,$$

where A_i^n, B_i^n and C_i^n are known. Similarly, from the other relations of (3.3), we get

$$\dot{P}_i^n = \overline{A}_i^n + \overline{B}_i^n\dot{K}_1^n + \overline{C}_i^n\dot{K}_2^n, \quad \dot{Q}_i^n = \widetilde{A}_i^n + \widetilde{B}_i^n\dot{K}_1^n + \widetilde{C}_i^n\dot{K}_2^n \quad \text{for} i=1,2.$$

Computing the discrete inner product of three relations mentioned above with X_i^n, Y_i^n and Z_i^n, respectively, for $i=1,2$, one has

$$\begin{cases} 2\mathrm{I}_i^n &= \langle\dot{\Phi}_i^n, X_i^n\rangle = \langle A_i^n, X_i^n\rangle + \langle B_i^n, X_i^n\rangle(\mathrm{I}_1^n+\mathrm{II}_1^n+\mathrm{III}_1^n) + \langle C_i^n, X_i^n\rangle(\mathrm{I}_2^n+\mathrm{II}_2^n+\mathrm{III}_2^n),\\ \mathrm{II}_i^n &= \langle\dot{P}_i^n, Y_i^n\rangle = \langle\overline{A}_i^n, Y_i^n\rangle + \langle\overline{B}_i^n, Y_i^n\rangle(\mathrm{I}_1^n+\mathrm{II}_1^n+\mathrm{III}_1^n) + \langle\overline{C}_i^n, Y_i^n\rangle(\mathrm{I}_2^n+\mathrm{II}_2^n+\mathrm{III}_2^n),\\ \mathrm{III}_i^n &= \langle\dot{Q}_i^n, Z_i^n\rangle = \langle\widetilde{A}_i^n, Z_i^n\rangle + \langle\widetilde{B}_i^n, Z_i^n\rangle(\mathrm{I}_1^n+\mathrm{II}_1^n+\mathrm{III}_1^n) + \langle\widetilde{C}_i^n, Z_i^n\rangle(\mathrm{I}_2^n+\mathrm{II}_2^n+\mathrm{III}_2^n). \end{cases}$$

We solve the linear algebraic equations and obtain the values of $\mathrm{I}_i^n, \mathrm{II}_i^n$ and III_i^n $(i=1,2)$. These results lead to the values of $\dot{K}_i^n$ and $\dot{P}_i^n$, $\dot{Q}_i^n$, $\dot{\Phi}_i^n$ sequentially. In terms of the iterative errors of P_i^n, Q_i^n and Φ_i^n, one could determine the values of $\dot{\Upsilon}_i^n$ $(\Upsilon = P, Q, \Phi, W, K)$ and finally get the numerical solutions at the next time level from (3.4) and update the iterative values.

Acknowledgements The authors would like to thank Prof. Yuezheng Gong from Nanjing University of Aeronautics and Astronautics for inspiring discussions on numerical computation. The authors would also like to thank the referees for their careful reading and constructive comments and suggestions which improve the quality of the manuscript.

Funding The first author is supported by a grant JZ2021HGQA0246 from the Fundamental Research Funds for the Central Universities.

Declarations

Competing interests The authors declare no competing interests.

References

1. Makhankov, V.G.: Dynamics of classical solitons (in non-integrable systems). Phys. Rep. **35**, 1–128 (1978)
2. Bao, W., Zhao, X.: A uniformly accurate (UA) multiscale time integrator fourier pseoduspectral method for the Klein-Gordon-SchröDinger equations in the nonrelativistic limit regime. Numer. Math. **135**, 833–873 (2017)
3. Fukuda, I., Tsutsumi, M.: On coupled Klein-Gordon-SchröDinger equations II. J. Math. Anal. Appl. **66**, 358–378 (1978)
4. Guo, B.: Global solution for some problem of a class of equations in interaction of complex SchröDinger field and real Klein-Gordon field. Sci. China A **25**, 897–910 (1982)

5. Ohta, M.: Stability of stationary states for the coupled Klein-Gordon-Schrödinger equations. Nonlinear Anal. **27**, 455–461 (1996)
6. Guo, B., Miao, C.: Global existence and asymptotic behavior of solutions for the coupled Klein-Gordon-Schrödinger equations. Sci. China A **38**, 1444–1456 (1995)
7. Bao, W., Dong, X., Wang, S.: Singular limits of Klein-Gordon-Schrödinger equations. Multiscale Model. Simul. **8**(5), 1742–1769 (2010)
8. Wang, M., Zhou, Y.: The periodic wave solutions for the Klein-Gordon-Schrödinger equations. Phys. Lett. A **318**, 84–92 (2003)
9. Wang, T.: Optimal point-wise error estimate of a compact difference scheme for the Klein-Gordon-Schrödinger equation. J. Math. Anal. Appl. **412**, 155–167 (2014)
10. Wang, T., Zhao, X., Jiang, J.: Unconditional and optimal h^2-error estimates of two linear and conservative finite difference schemes for the Klein-Gordon-Schrödinger equation in high dimensions. Adv. Comput. Math. **44**, 477–503 (2018)
11. Wang, J., Liang, D., Wang, Y.: Analysis of a conservative high-order compact finite difference scheme for the Klein-Gordon-Schrödinger equation. J. Comput. Appl. Math. **358**, 84–96 (2019)
12. Li, M., Shi, D., Wang, J., Ming, W.: Unconditional superconvergence analysis of the conservative linearized Galerkin FEMs for nonlinear Klein-Gordon-Schrödinger equation. Appl. Numer. Math. **142**, 47–63 (2019)
13. Kong, L., Liu, R., Xu, Z.: Numerical simulation of interaction between SchröDinger field and Klein-Gordon field by multisymplectic method. Appl. Math. Comput. **181**, 342–350 (2006)
14. Hong, J., Jiang, S., Li, C.: Explicit multi-symplectic methods for Klein-Gordon-SchröDinger equations. J. Comput. Phys. **228**, 3517–3532 (2009)
15. Bao, W., Yang, L.: Efficient and accurate numerical methods for the Klein-Gordon-SchröDinger equations. J. Comput. Phys. **225**, 1863–1893 (2007)
16. Hong, Q., Wang, Y., Wang, J.: Optimal error estimate of a linear fourier pseudo-spectral scheme for two dimensional Klein-Gordon-SchröDinger equations. J. Math. Anal. Appl. **468**, 817–838 (2018)
17. Wang, S., Zhang, L.: A class of conservative orthogonal spline collocation schemes for solving coupled Klein-Gordon-SchröDinger equations. Appl. Math. Comput. **203**, 799–812 (2008)
18. Griffiths, D.F., Higham, D.J.: Numerical methods for ordinary differential equations: initial value problems. Springer, Berlin (2010)
19. Cooper, G.J.: Stability of Runge-Kutta methods for trajectory problems. IMA J. Numer. Anal. **7**(1), 1–13 (1987)
20. Hairer, E., Lubich, C., Wanner, G.: Geometric numerical integration: structure-preserving algorithms for ordinary differential equations, vol. 31. Springer, Berlin (2006)
21. Calvo, M.P., Iserles, A., Zanna, A.: Numerical solution of isospectral flows. Math. Comput. **66**, 1461–1486 (1997)
22. Yang, X., Ju, L.: Efficient linear schemes with unconditional energy stability for the phase field elastic bending energy model. Comput. Methods Appl. Mech. Engrg. **315**, 691–712 (2017)
23. Yang, X., Zhao, J., Wang, Q.: Numerical approximations for the molecular beam epitaxial growth model based on the invariant energy quadratization method. J. Comput. Phys. **333**, 104–127 (2017)
24. Yang, X., Yu, H.: Efficient second order unconditionally stable schemes for a phase field moving contact line model using an invariant energy quadratization approach. SIAM J. Sci. Comput. **40**(3), B889–B914 (2018)
25. Shen, J., Xu, J., Yang, J.: The scalar auxiliary variable (SAV) approach for gradient flows. J. Comput. Phys. **353**, 407–416 (2018)
26. Shen, J., Xu, J.: Convergence and error analysis for the scalar auxiliary variable (SAV) schemes to gradient flows. SIAM J. Numer. Anal. **56**(5), 2895–2912 (2018)
27. Shen, J., Xu, J., Yang, J.: A new class of efficient and robust energy stable schemes for gradient flows. SIAM Rev. **61**(3), 474–506 (2019)
28. Gong, Y., Zhao, J.: Energy-stable Runge-Kutta schemes for gradient flow models using the energy quadratization approach. Appl. Math. Lett. **94**, 224–231 (2019)
29. Gong, Y., Zhao, J., Wang, Q.: Arbitrary high-order unconditionally energy stable schemes for thermodynamically consistent gradient flow models. SIAM J. Sci. Comput. **42**, B135–B156 (2020)
30. Gong, Y., Zhao, J., Wang, Q.: Arbitrarily high-order linear energy stable schemes for gradient flow models. J. Comput. Phys. **419**, 109610 (2020)

31. Jiang, C., Cai, W., Wang, Y.: A linearly implicit and local energy-preserving scheme for the Sine-Gordon equation based on the invariant energy quadratization approach. J. Sci. Comput. **80**(3), 1629–1655 (2019)
32. Li, H., Hong, Q.: An efficient energy-preserving algorithm for the Lorentz force system. Appl. Math. Comput. **358**, 161–168 (2019)
33. Jiang, C., Wang, Y., Gong, Y.: Arbitrarily high-order energy-preserving schemes for the Camassa-Holm equation. Appl. Numer. Math. **151**, 85–97 (2020)
34. Li, X., Gong, Y., Zhang, L.: Linear high-order energy-preserving schemes for the nonlinear SchröDinger equation with wave operator using the scalar auxiliary variable approach. J. Sci. Comput. **88**, 20 (2021)
35. Fukuda, I., Tsutsumi, M.: On the Yukawa-coupled Klein-Gordon-SchröDinger equations in three space dimensions. Proc. Jpn. Acad. **51**, 402–405 (1975)
36. Wang, B., Lange, H.: Attractors for the Klein-Gordon-SchröDinger equation. J. Math. Phys. **40**, 2445–2457 (1999)
37. Gong, Y., Wang, Q., Wang, Y., Cai, J.: A conservative Fourier pseudo-spectral method for the nonlinear SchröDinger equation. J. Comput. Phys. **328**, 354–370 (2017)
38. Zhang, Z., Gong, Y., Zhao, J.: A remark on the invariant energy quadratization (IEQ) method for preserving the original energy dissipation laws, arXiv:2111.12920v1 (2021)
39. Zhao, J.: A revisit of the energy quadratization method with a relaxation technique. Appl. Math. Lett. **120**, 107331 (2021)
40. Jiang, M., Zhang, Z., Zhao, J.: Improving the accuracy and consistency of the scalar auxiliary variable (SAV) method with relaxation. J. Comput. Phys. **456**, 110954 (2022)
41. Cheng, Q., Liu, C., Shen, J.: A new Lagrange multiplier approach for gradient flows. Comput. Methods Appl. Mech. Engrg. **367**, 113070 (2020)
42. Gong, Y., Hong, Q., Wang, Q.: Supplementary variable method for thermodynamically consistent partial differential equations. Comput. Methods Appl. Mech. Engrg. **381**, 113746 (2021)